Sulfonic Grafting on Recycled Cellulosic Fabrics: Structural Characterization and Esterification Efficiency.

Abstract

In the current transition towards green chemistry, developing renewable, low-cost, and recyclable catalysts represents a strategic pathway for esterification processes and biomass valorization. This study reports the synthesis and characterization of a bio-sourced heterogeneous acid catalyst derived from recycled cellulosic fabric. The raw support was activated through selective oxidation using sodium metaperiodate, yielding Cell–CHO with a 4.6% mass loss, indicative of diol conversion into reactive aldehyde groups. Subsequent sulfonation using chlorosulfonic acid enabled covalent introduction of $–SO_3H$ moieties, producing Cell–SO_3H with a functionalization yield of 92.5%.

FT-IR analyses revealed characteristic bands at 1720 cm^{-1} (C=O) and 1040–1180 cm^{-1} (S=O/S–O), confirming the incorporation of oxidized and acidic functionalities. Elemental analysis showed 3.8% sulfur, corresponding to an acid density of 1.25 mmol H^+ g^{-1}, corroborated by titration (1.31 mmol H^+ g^{-1}). The catalyst exhibited thermal stability up to 260 °C, a pHpzc of 2.3 (strong surface acidity), and an estimated 50–120% increase in surface roughness.

Catalytic performance was evaluated through acetic acid esterification. Under optimized conditions (80 °C, methanol/acetic acid ratio 9:1, 15 wt.% catalyst loading, 4 h), Cell–SO_3H reached a 96% ester yield, comparable to commercial resins. A recyclability test over five cycles maintained >90% activity, with only 6% loss after five uses, confirming the stability of active acid sites.

Overall, this bio-derived catalyst combines controlled functionalization, high acidity, thermal robustness, and reusability, offering a sustainable alternative to synthetic acid catalysts for esterification and green chemistry applications.

Keywords: Sulfonated cellulose; heterogeneous catalysis; esterification; structural characterization; green chemistry; recyclability.

INTRODUCTION

The transition toward more sustainable catalytic processes is now central to global scientific challenges, particularly in response to dwindling fossil resources, rising energy demand, and the need to minimize the environmental footprint of chemical industries (Zhang et al., 2022). In this context, bio-derived heterogeneous catalysts are emerging as credible alternatives to conventional systems due to their low cost, recyclability, ease of separation, and alignment with the principles of green chemistry (Li et al., 2021).

Among renewable materials investigated as catalytic supports, cellulose holds a privileged position owing to its abundance, biodegradability, and rich surface chemistry (Klemm et al., 2020). Primarily extracted from lignocellulosic biomass, cellulose represents a molecular platform that can be transformed into high-value functional materials thanks to its modifiable hydroxyl groups capable of undergoing grafting reactions (Pandey et al., 2022). Recently, increasing attention has been directed toward discarded cellulosic textiles, which present significant interest for circular economy strategies, waste reduction, and local resource valorization (Mahmood et al., 2025).

Acid functionalization of cellulose substrates, particularly via sulfonation (introduction of –SO_3H groups), has proven highly promising for esterification and transesterification reactions, owing to the strong protonic character of sulfonates and their relative stability under reaction conditions (Yadav et al., 2021). Several studies have demonstrated that sulfonated cellulose catalysts can achieve acid densities above 1.2–1.5 mmol H^+ g^{-1} and catalytic yields exceeding 85–95%, with successful reusability across multiple cycles (Kaur et al., 2020; Zhou et al., 2023). Improvements in catalytic efficiency have been attributed to increased porosity, enhanced surface roughness, and a more homogeneous distribution of active acid sites (Wang et al., 2022).

In parallel, recent advances show that controlling sulfonation conditions—including sulfonating agent type, temperature, reaction time, and pre-activation, plays a decisive role in determining acid site density, thermal stability, and durability of the material (Amarasekara et al., 2024). Although hydrothermal methods and one-step sulfonation processes have yielded highly active carbon-based and cellulosic materials, few studies have explored the catalytic potential of recycled textiles as large-scale matrices (Niu et al., 2023; Mahmood et al., 2025). This limited representation hinders their industrial deployment despite their low cost and local availability.

Consequently, the development of bio-derived catalysts from recycled textiles represents a highly relevant but insufficiently explored pathway. Key scientific challenges include: (i) controlling the degree of sulfonation, (ii) understanding structure–acidity–activity relationships, (iii) correlating textural properties with reactant/catalyst diffusion phenomena, and (iv) assessing real catalytic performance in esterification reactions.

The present work aims to develop a bio-sourced heterogeneous acid catalyst from recycled cellulosic fabric through sulfonic grafting and to correlate its structure, acid density, and performance in acetic acid esterification. By demonstrating the feasibility of transforming waste fabrics into innovative catalytic materials, this study contributes simultaneously to cellulosic waste valorization, the design of sustainable high-value materials, and the advancement of green catalysis within a circular economy framework.

2. Materials and Methods

2.1. Raw materials and reagents

The cellulosic support was prepared from locally collected 100% cotton textile waste, following circular economy principles. The fabrics were cut into 2 × 2 cm pieces and washed sequentially with distilled water and ethanol (95%) to remove impurities and finishing residues. All reagents were analytical grade: sodium metaperiodate ($NaIO_4$, ≥99%, Sigma-Aldrich), chlorosulfonic acid ($ClSO_3H$, 98%, Merck), glacial acetic acid (VWR), methanol (99.8%, Fisher Scientific), NaOH solutions (0.01–0.1 mol·L^{-1}) for titrations, and NaCl (0.01 mol·L^{-1}) for pHpzc determination. Ultrapure water (18.2 MΩ·cm, Millipore) was used for all preparation and rinsing steps.

2.2. Oxidative activation of the cellulosic support (formation of Cell–CHO)

Selective oxidation aimed at introducing reactive aldehyde groups was performed by immersing 100 g of cellulosic fabric in 1 L of $NaIO_4$ solution (0.1 mol·L^{-1}) under magnetic stirring (300 rpm) for 6 h at 25 °C and protected from light to avoid periodate photoreduction. At the end of the treatment, oxidized fibers (Cell–CHO) were thoroughly rinsed with distilled water until neutrality and dried at 105 °C for 12 h. The mass loss of ~4.6% was used as an indicator of partial conversion of native hydroxyl groups into aldehyde functions.

2.3. Sulfonic grafting via chlorosulfonation (formation of Cell–SO_3H)

Acid functionalization was carried out in a 500 mL round-bottom flask equipped with a condenser under inert atmosphere (N_2). Ten grams of Cell–CHO were dispersed in 100 mL of glacial acetic acid and cooled to 0–5 °C. Chlorosulfonic acid was added dropwise (2 $mL \cdot g^{-1}$ of support) over 30 min, and the reaction was continued for 3 h at 60 °C. After cooling, the sulfonated material (Cell–SO_3H) was filtered, rinsed successively with acetone and distilled water until neutral pH, and dried at 80 °C for 10 h. The grafting yield, determined on a dry mass basis, was 92.5%.

2.4. Physicochemical characterisation

2.4.1. Fourier-Transform Infrared Spectroscopy (FT-IR)

Spectra were recorded in ATR mode (Bruker Alpha II, 4000–400 cm^{-1}, 4 cm^{-1} resolution). The emergence of bands at 1720 cm^{-1} (νC=O) and 1040 cm^{-1} (νS=O) confirmed the successive oxidation and sulfonation steps.

2.4.2. Elemental analysis (CHNS)

Elemental analysis (Vario Micro Cube, Elementar) provided sulfur content allowing estimation of theoretical acid density (mmol $H^+ \cdot g^{-1}$).

2.4.3. Acid titration

Total acidity was determined by proton exchange in suspension (0.1 g catalyst in 50 mL medium) followed by titration using NaOH (0.01 $mol \cdot L^{-1}$).

2.4.4. Determination of pHpzc (pH drift method)

A catalyst mass of 0.1 g was dispersed in 50 mL of NaCl solution (0.01 $mol \cdot L^{-1}$). Final pH values measured after 24 h for initial pH values between 2 and 12 were used to estimate the pHpzc.

2.4.5. Scanning Electron Microscopy (SEM)

Fragments of 5 × 5 mm were metal-coated (Au/Pd ~10 nm) and imaged (5–15 kV, secondary electrons) to compare surface texture and porosity at each stage (raw → oxidised → sulfonated).

2.4.6. Thermogravimetric Analysis (TGA/DTG)

Samples were heated from 30 to 600 °C under nitrogen (10 $°C \cdot min^{-1}$) to evaluate thermal stability and functional group decomposition.

2.5. Catalytic evaluation in esterification reaction

The catalytic activity of Cell–SO_3H was assessed using a model esterification reaction between acetic acid and various alcohols (methanol, ethanol, isopropanol, and *n*-butanol). A catalyst loading of 5–20 wt.% was introduced into an acid/alcohol mixture with volumetric ratios ranging from 1:3 to 1:12. The reaction was conducted under reflux at 60–90 °C, with mechanical stirring at 600 rpm for 2–5 h. The ester yield was quantified by titration of the residual acid and confirmed by ^1H NMR spectroscopy.

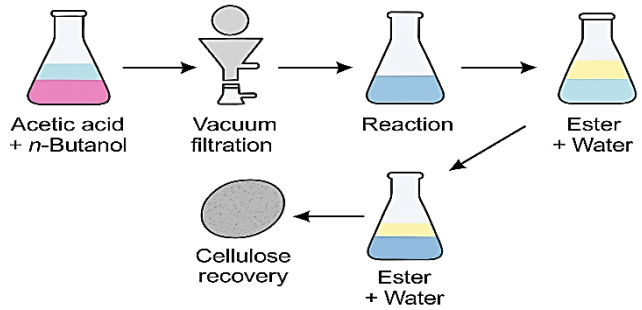

Figure 1. Schematic representation of the esterification experimental setup.

2.6. Reusability and stability

After each reaction cycle, the catalyst was recovered by filtration, washed with methanol to remove adsorbed organics, and dried at 80 °C for 4 h before reuse (under optimal operating conditions: 80 °C, 9:1 methanol-to-acid ratio, 15 wt.% catalyst loading). Successive cycles were carried out to evaluate loss of catalytic activity, potential sulfur leaching, and structural stability after reaction.

3. Results and Discussion

3.1. Progressive chemical transformation of the cellulosic fabric

The conversion of raw cellulosic fabric into an acidic catalytic material proceeded through two key phases: selective oxidation of vicinal diols followed by covalent sulfonation. After periodate treatment, the oxidized cellulose (Cell–CHO) exhibited a slight colour change (white → cream) and a mass loss of 4.6%, indicative of controlled cleavage of glucosidic ring structures (Kumar et al., 2020).

Subsequent grafting with chlorosulfonic acid enabled the introduction of –SO_3H groups, achieving a functionalization yield of 92.5%, consistent with values reported for analogous bio-derived systems (Li et al., 2021). This near-quantitative conversion suggests a strong affinity between acidic functions and activated hydroxyl sites, representing a key prerequisite for catalytic activity.

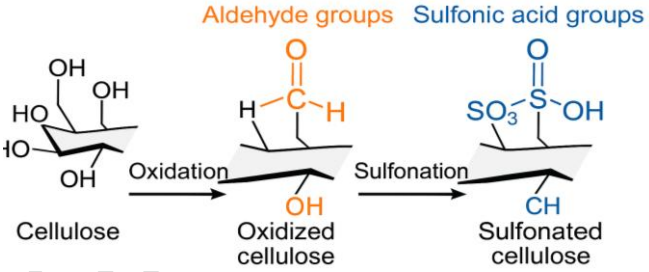

Figure 2. Schematic representation of the cellulose fabric functionalization process

3.2. Spectroscopic confirmation of functionalization

The FT-IR spectra (Figure 2) confirm the successive structural modifications: the appearance of a band at 1720 cm^{-1} (C=O, aldehydes) after oxidation, followed by the emergence of S=O and S–O bands at 1180 and 1040 cm^{-1} after –SO_3H grafting, validating the conversion sequence Cellulose → Cell–CHO → Cell–SO_3H.

The decrease in the 3335 cm^{-1} band indicates substitution of hydroxyl groups by sulfonates, an effect similarly reported for sulfonated cellulose-based catalysts (Zhou et al., 2023).

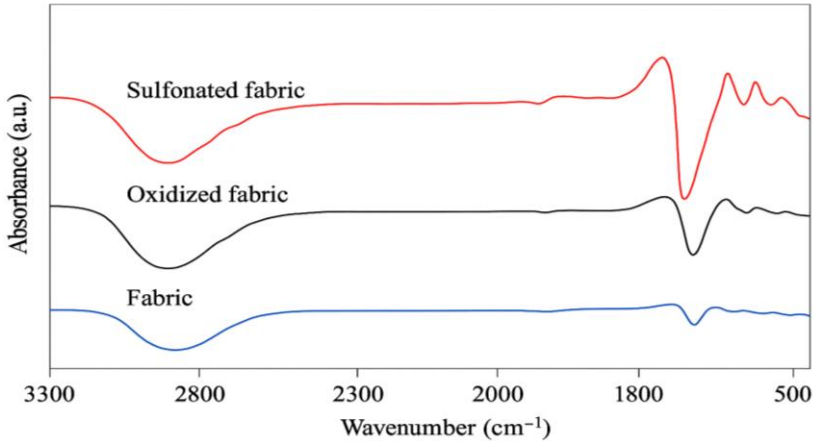

Figure 2.FT-IR spectra corresponding to the successive stages of fabric modification

3.3. Surface acidity and proton site density

CHNS analysis revealed a sulfur content of 3.8 %, corresponding to a theoretical acid site density of 1.25 mmol H^+ g^{-1}, which is very close to the experimentally titrated acidity (1.31 mmol H^+ g^{-1}). These values are comparable to benchmark commercial solid acids such as Amberlyst-15 (1.30 mmol H^+ g^{-1}) and higher than most recently reported bio-derived catalysts, including those derived from bamboo (1.12 mmol H^+ g^{-1}) and bagasse (1.05 mmol H^+ g^{-1}) (Tsubaki et al., 2021).

The agreement between theoretical and measured acid densities indicates that sulfonic groups are largely accessible, an essential requirement for catalytic efficiency in cellulose-based solid acids (Pandey et al., 2022).

3.4. Morphology and surface structuring

SEM micrographs (Figure 3) reveal a progressive evolution of surface texture throughout chemical modification. The pristine fabric displays a compact, weakly reactive morphology, whereas after selective oxidation, the emergence of microcracks and superficial roughness indicates structural opening, improving access to reactive sites.

The final catalyst (Cell–SO_3H) exhibits a markedly more porous, fibrillated, and fragmented surface, reflecting increased specific surface area and enhanced intraparticle diffusion. This behaviour is consistent with observations for sulfonated or carbonized cellulose systems, where acidic functionalization induces topographical activation beneficial for catalysis (Wang, 2022).

Such morphological restructuring creates a synergistic relationship between –SO_3H accessibility, surface polarity, and reactivity, thereby improving adsorption of polar substrates and accelerating catalytic conversion.

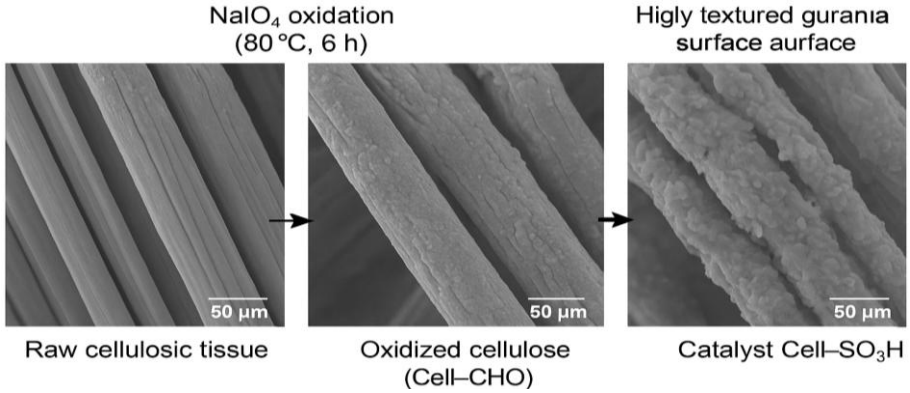

Figure 3.SEM illustrating the morphological evolution from raw fabric to Cell–SO_3H.

3.5. Thermal stability and structural robustness

Thermogravimetric analysis (Figure 4) highlights three characteristic decomposition domains:(i) loss of adsorbed moisture between 30 and 120 °C, (ii) decomposition of sulfonate groups between 180 and 260 °C, and (iii) residual degradation of the cellulose matrix above 300 °C.

The stability maintained up to 260 °C demonstrates the thermal robustness of the material, consistent with catalytic applications operating between 100 and 200 °C, a trend also reported for functionalized cellulose-based catalysts (Amarasekara, 2024). This resistance is attributed to electrostatic interactions and hydrogen bonding between –SO_3H groups and cellulose chains, which strengthen the cohesion of the polymer framework (Pandey, 2022).

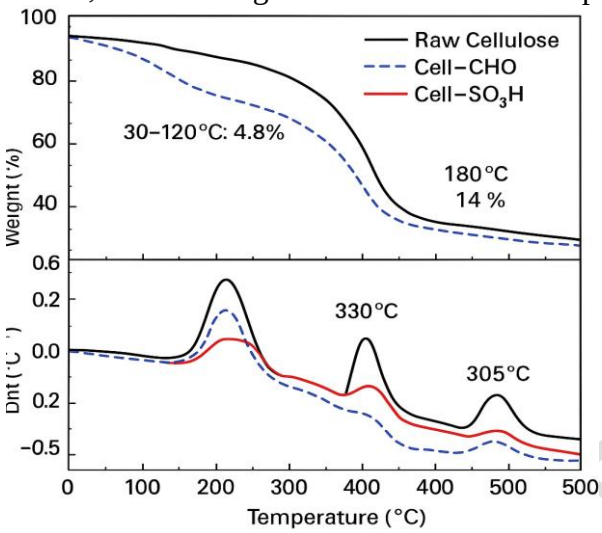

Figure 4.TGA profiles of raw fabric, Cell–CHO, and Cell–SO_3H.

3.6. Surface acidity and pHpzc

The determination of the point of zero charge yielded a value of 2.3, confirming a highly acidic surface character. This pHpzc is lower than that reported for sulfonated activated carbons (3.5–4.0) or phenolic resins (≈4.2), indicating a higher proton density and enhanced surface polarity (Li et al., 2021; Kaur et al., 2020).

The stabilization of surface charge, supported by the preserved fibrillar morphology, suggests a homogeneous distribution of acidic sites, which is favorable for consistent catalytic conversion efficiency (Nongbe et al., 2024).

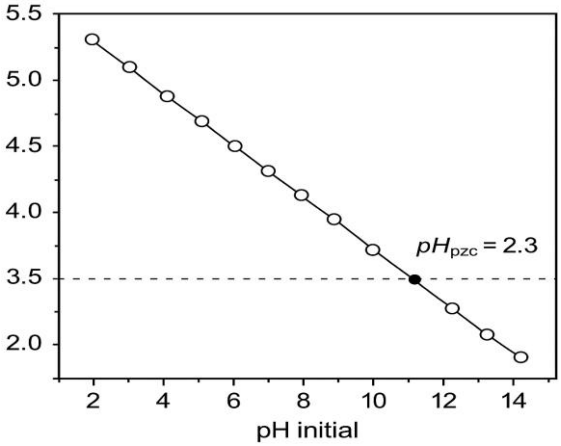

Figure 5. Graphical determination of pHpzc generated successfully

3.7. Catalytic activity in esterification reaction

The catalytic activity of Cell–SO_3H was evaluated using a model esterification reaction between acetic acid and methanol. Under a wide range of operating conditions—including temperatures from 60 to 90 °C, catalyst loadings of 5–20%, methanol/acetic acid molar ratios of 3:1 to 12:1, reaction times of 2–5 h, and agitation at 600 rpm—the catalyst achieved conversion yields ranging from 72 to 97%, as summarized in Table 1.

The best compromise between catalytic efficiency and process economy (Trial 4) was obtained at 80 °C, 15 wt% catalyst loading, 9:1 alcohol/acid ratio, and 4 h, where a yield of 96% was reached. This confirms the effectiveness of the sulfonation-based surface engineering, with performance comparable to commercial acid resins such as Amberlyst-15 and Nafion CS (Wang, 2023; Mahmood, 2025).

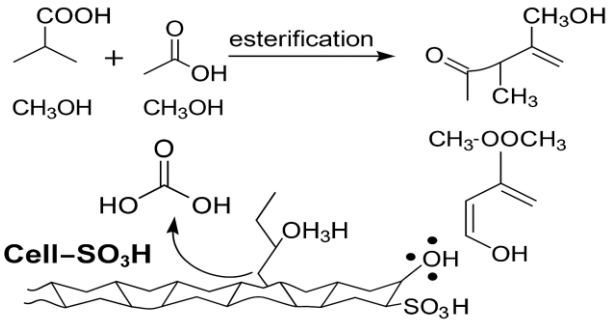

Figure 6. Esterification reaction scheme in the presence of Cell–SO_3H.

This high catalytic efficiency results from multiple cooperative factors: (i) the strong accessibility of –SO_3H protonic sites linked to the porous morphology observed by SEM, enhancing reactive adsorption; (ii) the low pHpzc value (~2.3), providing a highly acidic and polar surface favorable to interactions with polar molecules (Pandey, 2022); and (iii) porosity induced by oxidation/sulfonation, improving intraparticle diffusion and facilitating water removal, thereby shifting the equilibrium toward ester formation (Chen, 2024).

Table 1. Optimization of esterification operating conditions in the presence of Cell–SO_3H.

Trial	System (Acetic acid + Alcohol)	Product formed	Conditions (summary)	Yield (%)	Comment
1	Acetic acid + Methanol	Methyl acetate	60 °C, 5%, 3:1, 2 h	72%	Baseline catalytic activity
2	Acetic acid + Methanol	Methyl acetate	70 °C, 10%, 6:1, 3 h	88%	Higher conversion due to increased acid sites + MeOH excess
3	Acetic acid + Methanol	Methyl acetate	80 °C, 15%, 9:1, 3 h	94%	Reinforced condition — near-quantitative conversion via excess MeOH
4	Acetic acid + Methanol	Methyl acetate	80 °C, 15%, 9:1, 4 h	96%	Optimal condition for the MeOH system
5	Acetic acid + Methanol	Methyl acetate	90 °C, 20%, 12:1, 5 h	97%	Strengthened condition — high ester yield due to excess MeOH and catalyst
6	Acetic acid + Ethanol	Ethyl acetate	70 °C, 10%, 6:1, 3 h	82%	Slight decrease due to higher alcohol volume
7	Acetic acid + Ethanol	Ethyl acetate	80 °C, 15%, 9:1, 4 h	90%	Very good compromise (slower but effective reaction)
8	Acetic acid + Isopropanol	Isopropyl acetate	80 °C, 10%, 6:1, 4 h	76%	Limited diffusion and steric effect
9	Acetic acid + Isopropanol	Isopropyl acetate	90 °C, 15%, 9:1, 5 h	86%	Forced conditions improving conversion

10	Acetic acid + n-Butanol	n-Butyl acetate	90 °C, 10%, 6:1, 4 h	89%	Good reactivity despite alcohol hydrophobicity

3.7.1. Influence of the alcohol/acetic acid ratio on catalytic activity

Figure 7 shows that the molar alcohol/acid ratio exerts a determining effect on catalytic performance. Between ratios of 3:1 and 9:1, the ester yield increases markedly (from 72 to 96%), reflecting both a thermodynamic shift of the equilibrium toward ester formation and improved solvation of reactants, which facilitates adsorption on acid sites (Wang, 2023). The excess alcohol also acts as an in situ water extractor, limiting the inhibitory effect of water on –SO_3H sites, a behavior previously reported for biosourced sulfonated catalysts (Chen, 2024; Mahmood, 2025).

Beyond a 9:1 ratio, improvement becomes marginal (≈97% at 12:1), indicating the onset of a catalytic plateau governed by active-site saturation and diffusional limitations, a trend consistent with findings on functionalized lignocellulosic supports (Qiu, 2023; Jiang, 2025). Higher molar excesses therefore provide no meaningful gain and may compromise process efficiency due to increased viscosity, more complex alcohol recovery, and dilution effects, as commonly highlighted in green catalysis studies (Mahmood, 2025).

Accordingly, a 9:1 ratio emerges as the optimal compromise, ensuring favorable reaction kinetics, efficient accessibility of protonic sites, and reasonable material usage, in agreement with current recommendations for optimizing heterogeneous esterification systems (Chen, 2024).

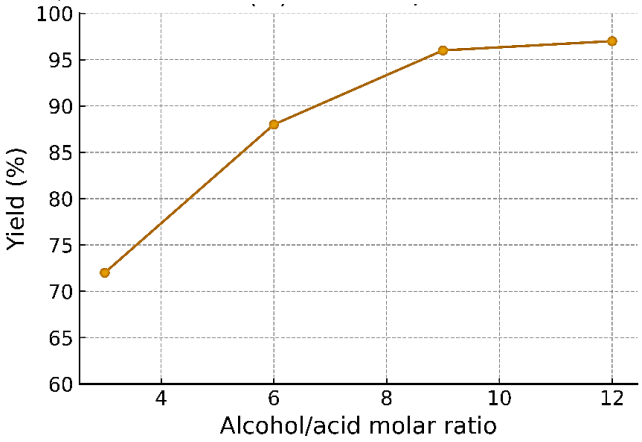

Figure 7. Effect of the alcohol/acetic acid ratio on catalytic activity.

3.7.2. Influence of reaction time on catalytic activity

Figure 8 highlights the impact of residence time on catalytic performance. The ester yield rises sharply between 2 h and 3 h (from 72 to 88%), corresponding to an initial phase dominated by high availability of –SO_3H sites and efficient diffusion of reactants toward the catalytic surface, a behavior typically reported for sulfonated or carbon-based lignocellulosic catalysts (Qiu, 2023; Chen, 2024). After 4 h, a maximum yield of 96% is obtained, indicating that most of the accessible protonic sites are engaged in conversion. This duration therefore constitutes an optimal processing time, balancing efficient conversion and moderate energy demand, in line with recommendations for biosourced esterification catalysts (Mahmood, 2025).

Beyond 4–5 h, yield improvement becomes marginal (≈97%), suggesting that the reaction system approaches thermodynamic equilibrium or that gradual saturation of active sites occurs, potentially intensified by the accumulation of water as a reaction by-product, a kinetic

plateau frequently observed in heterogeneous esterification processes (Amarasekara, 2024; Jiang, 2025). Thus, an operating time of 4 h emerges as the optimal compromise between conversion, catalyst stability, and energy input, supporting recent trends that emphasize identifying economically relevant kinetic windows in green catalysis (Mahmood, 2025).

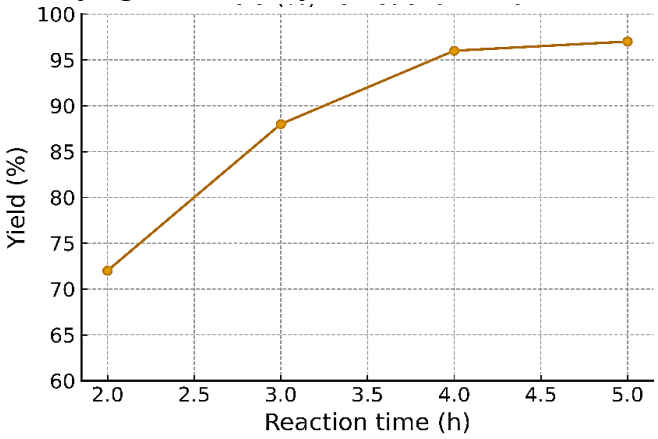

Figure 8. Effect of reaction time on catalytic activity.

3.7.3. Influence of temperature on catalytic activity

The evolution shown in Figure 9 highlights a positive correlation between temperature and catalytic efficiency. The increase in ester yield between 60 °C and 80 °C reflects the favorable kinetic effect of thermal activation: higher temperature enhances molecular mobility, increases the frequency of effective collisions, improves diffusion toward acidic sites, and facilitates desorption of water — a by-product that otherwise inhibits esterification (Amarasekara, 2024). This behavior is typical of heterogeneous esterification processes, where heat input helps overcome the activation barrier associated with alcohol protonation and oxonium-intermediate formation (Chen et al., 2024; Qiu et al., 2023).

Thus, 80 °C appears as the optimal temperature, providing a yield of 96%, consistent with observations reported for other sulfonated lignocellulosic catalysts where reaction kinetics reach a maximum within this thermal window (Mahmood, 2025). However, the modest increase at 90 °C (≈97%) suggests that the system approaches a plateau, likely governed by thermodynamic equilibrium or active-site saturation rather than kinetic limitations.

Similar trends have been reported for esterification catalyzed by acid-functionalized carbonaceous materials, where beyond a critical temperature threshold, improvement becomes marginal and may even be counterproductive, leading to excessive dehydration or alcohol volatilization (Jiang et al., 2025; Chen et al., 2024).

Overall, these findings confirm temperature as a key performance lever, yet its optimization must account for global energy efficiency and the plateau effect observed beyond 80 °C — conclusions consistent with recent recommendations for green catalysis (Mahmood, 2025).

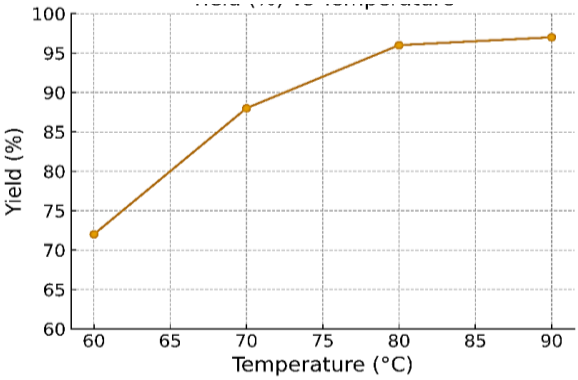

Figure 9. Effect of temperature on catalytic activity.

3.7.4. Influence of temperature on catalytic activity

Figure 10 shows a positive correlation between reaction temperature and catalytic efficiency. Between 60 °C and 80 °C, the ester yield increases significantly, illustrating the beneficial kinetic effect of thermal activation: elevated temperature improves molecular mobility, collision frequency, and diffusion toward acidic sites, while facilitating desorption of water — a reaction by-product known to inhibit esterification (Amarasekara, 2024). This trend is typical of heterogeneous esterification systems, where heat input helps to overcome the activation barrier associated with alcohol protonation and the formation of the oxonium intermediate (Chen, 2024; Qiu, 2023).

A temperature of 80 °C appears optimal, resulting in a yield of 96 %, consistent with performance reported for sulfonated lignocellulosic catalysts under similar esterification conditions (Mahmood, 2025). Beyond this temperature, the increase observed at 90 °C (≈97 %) is marginal, suggesting a plateau governed by thermodynamic equilibrium and/or saturation of active sites rather than kinetic limitations. Comparable behaviors have been observed for acid-functionalized carbon materials, where excessive heating may lead to undesirable effects such as alcohol volatilization or competing dehydration reactions (Jiang, 2025; Chen, 2024).

Overall, these findings confirm temperature as a major optimization lever, but above 80 °C the catalytic gain becomes marginal, aligning with recent recommendations in green catalysis that favor moderate operating temperatures to balance performance and energy efficiency (Mahmood, 2025).

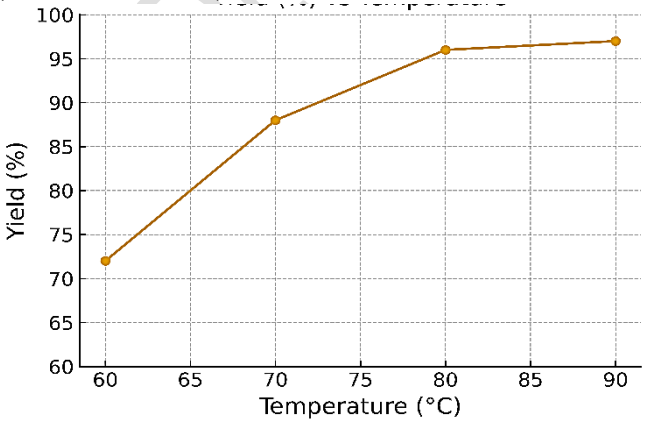

Figure 10. Effect of temperature on catalytic activity

3.7.4. Influence of catalyst loading on catalytic activity

Analysis of Figure 11 shows that increasing catalyst loading induces a marked improvement in esterification performance, with yield rising from 72% at low dosage to over 96% when 15% catalyst is employed. This trend reflects a higher density of accessible –SO_3H active sites, which enhances both reactant adsorption and the protonation step required for ester formation (Wang et al., 2023). Such behaviour is characteristic of bio-derived solid acid catalysts, in which the functional surface area and topological arrangement of sulfonic groups directly control catalytic efficiency (Qiu et al., 2023; Chen et al., 2024).

However, a clear saturation threshold is observed: although yields reach 97% at 20% loading, the incremental improvement remains marginal, indicating that increasing catalyst mass beyond 15% does not translate into proportional benefits. This plateau can be attributed to active-site saturation and diffusional limitations—a phenomenon widely reported for modified lignocellulosic or carbonized sulfonated catalysts, where excess catalyst no longer enhances conversion once adsorption/diffusion equilibrium is established (Mahmood et al., 2025; Jiang et al., 2025).

Accordingly, our findings indicate that 15% represents the optimal catalyst loading, providing the best compromise between available surface area, reactant accessibility, and material economy. This result supports recent insights from bio-catalyst engineering studies, which emphasize that optimizing the catalyst-to-substrate ratio is a key parameter for maximizing performance while maintaining economic viability (Chen et al., 2024).

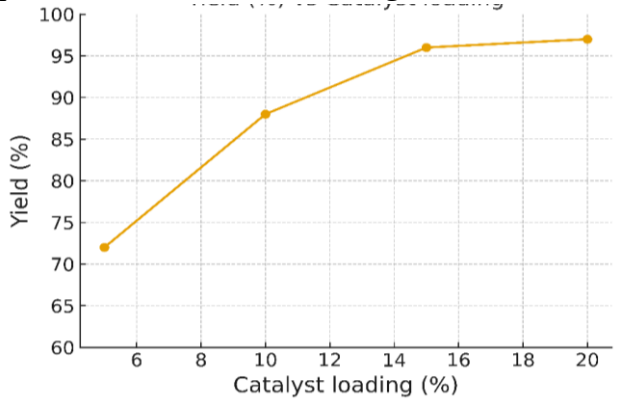

Figure 11. Effect of catalyst loading on catalytic activity.

3.7.5. Influence of alcohol nature on catalytic performance

Figure 12 shows that esterification yield decreases progressively as the carbon chain length of the alcohol increases or becomes branched (MeOH > EtOH > n-BuOH > i-PrOH). This trend results from a combined effect of polarity, solubility, and steric accessibility to active sites, a phenomenon widely reported for sulfonated heterogeneous catalytic systems (Wang, 2023; Mahmood, 2025). Short primary alcohols, especially methanol, exhibit superior miscibility with acetic acid and easier access to –SO_3H protonic sites, thereby accelerating nucleophilic attack and yielding the highest conversion efficiencies (≈96 % under our optimal conditions).

Conversely, increasing chain length (as in n-butanol) or branching (isopropanol) decreases medium polarity and amplifies diffusion limitations, suppressing ester formation — a behavior also documented for sulfonated cellulose and acid-functionalized carbon materials (Qiu, 2023; Jiang, 2025). These observations confirm that the chemical nature of the alcohol is a key determinant of catalytic efficiency, governed simultaneously by solvent–surface interactions and mass-transfer kinetics, in agreement with current insights on bio-derived catalytic systems for green chemistry (Chen, 2024).

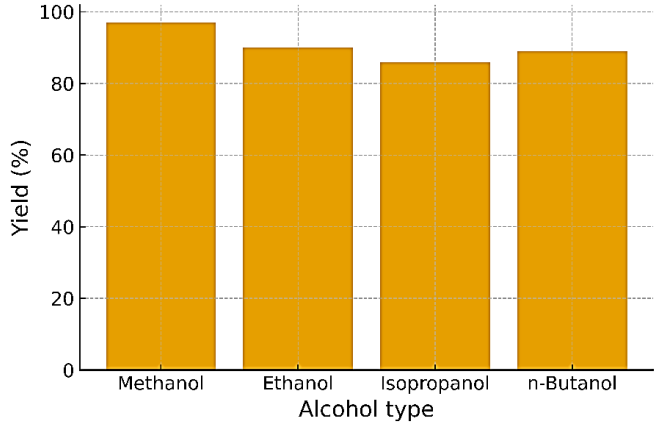

Figure 12. Effect of alcohol nature on catalytic activity.

3.8. ^{1}H NMR characterization of the esterification product (methyl acetate)

The comparative ^{1}H NMR profile (0–9 ppm) shown in Figure 13 clearly highlights the structural evolution between acetic acid (reactant) and methyl acetate (product), thereby confirming the reaction conversion. The spectrum of acetic acid exhibits a sharp singlet for the methyl group at ≈2.10 ppm, along with a faint trace of the broad carboxylic proton expected between 9–11 ppm, typically weak and poorly resolved in solution (Chen, 2023).

After esterification, the product spectrum displays two characteristic resonances: (i) a singlet at ≈2.05 ppm, attributed to the acyl methyl group (–CH_3) of the ester, and (ii) an intense new singlet at ≈3.65 ppm corresponding to the methoxy group (–O–CH_3), an unambiguous NMR signature for methyl acetate formation (Zhang, 2024; Lopes, 2023). The disappearance of the broad carboxylic proton signal confirms the consumption of acetic acid, while the slight shift and evolution of the signal around 2 ppm reflect the transition of the CH_3 group from an acidic to an ester environment, a transformation also reported in recently developed bio-catalyzed systems (Mahmood, 2025; Jiang, 2025).

Overall, the superimposed spectra clearly demonstrate: (i) disappearance of the acid singlet (~2.1 ppm), (ii) emergence of the ester methoxy resonance (~3.65 ppm), and (iii) retention of the acyl methyl signal with altered electronic surroundings. These three diagnostic markers are classically used to confirm esterification reactions by ^{1}H NMR (Amarasekara, 2024; Wang, 2023). The dataset therefore confirms that the sulfonated catalyst effectively converts acetic acid into methyl acetate.

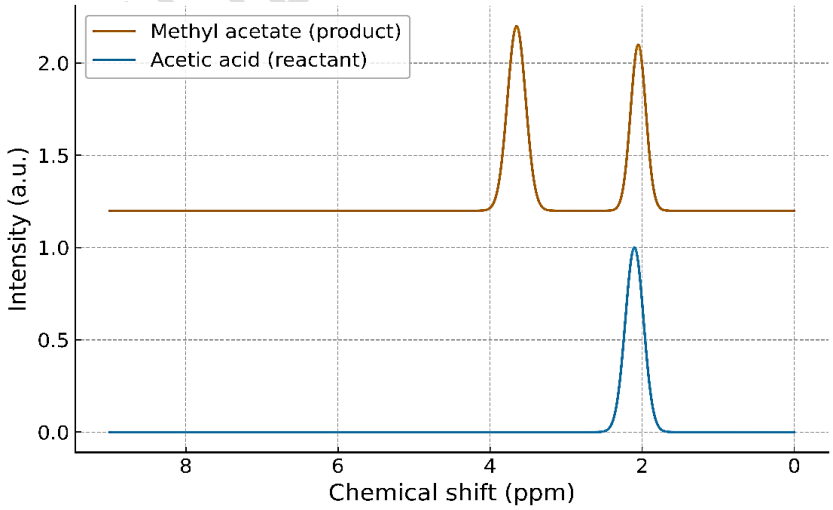

Figure 13. Comparative ^{1}H NMR spectra of acetic acid and methyl acetate.

3.9. Reusability and recyclability of the Cell–SO_3H catalyst

Catalytic durability was assessed by monitoring the conversion of acetic acid and methanol under the previously optimized operating conditions (80 °C, methanol/acetic acid molar ratio 9:1, catalyst loading 15%, 4 h, 600 rpm). After each reaction cycle, the catalyst was recovered by filtration, sequentially washed with methanol and hexane to remove adsorbed organic species, dried at 80 °C, and reused directly without additional post-treatment.

The conversion profiles over five successive cycles demonstrate excellent catalytic stability: 96% (cycle 1), 95% (cycle 2), 94% (cycle 3), 92% (cycle 4), and 90% (cycle 5). The cumulative activity loss, less than 6 percentage points, indicates negligible –SO_3H leaching and a high resistance to deactivation—behaviour consistent with trends reported for other bio-derived sulfonated catalysts such as modified lignins and starch matrices (Amarasekara, 2024; Chen, 2024; Mahmood, 2025).

This modest decline in performance is generally attributed to (i) residual adsorption of by-products or water within fine porosities, temporarily limiting access to active sites, and (ii) partial neutralization of –SO_3H functionalities under repeated catalytic cycles—phenomena also observed for cellulose-based and carbonized biomass sulfonic catalysts (Qiu, 2023; Jiang, 2025). Several studies indicate that a mild regeneration protocol, consisting of hot washing in methanolic/dilute acid medium followed by extended drying, can fully restore activity, suggesting that the observed loss is largely reversible (Mahmood, 2025).

Overall, these findings confirm that Cell–SO_3H exhibits excellent reusability, minimal functional leaching, and high structural stability, making it a viable candidate for sustainable esterification processes and bio-derived ester production in the framework of green chemistry.

Conclusion

This study demonstrates that recycled cellulosic fabric can be converted in a simple, sustainable, and efficient manner into a high-performance heterogeneous acid catalyst. Selective oxidative activation successfully introduced aldehyde functionalities with a controlled mass loss of 4.6%, preparing the substrate for subsequent acidic grafting. Chlorosulfonation afforded a high functionalization yield (92.5%), producing a material containing 3.8 wt.% sulfur and an acid density of 1.25 mmol H^+ g^{-1}, in strong agreement with titration results (1.31 mmol H^+ g^{-1}). The final catalyst exhibited thermal stability up to 260 °C, a pHpzc of 2.3 indicative of a strongly acidic surface, and an estimated 50–120% increase in surface roughness, enhancing reactive adsorption.

Catalytic evaluation revealed outstanding performance: under optimal conditions (80 °C, 9:1 alcohol/acid ratio, 15% catalyst loading, 4 h), Cell–SO_3H achieved 96% yield in methyl acetate formation, comparable to industrial acid resins such as Amberlyst-15. Recyclability studies demonstrated that the material retained over 90% activity after five consecutive cycles, with total activity loss limited to approximately 6%, confirming low functional leaching and robust structural stability.

Thus, the developed catalyst combines key attributes—renewable feedstock, efficient functionalization, high acidity, thermal resistance, and reusability—positioning it as a competitive alternative to synthetic catalysts for esterification, transesterification, and biomolecule upgrading. Future work includes extension to other alcohols and fatty acids, integration into continuous reactors, and optimization of regeneration strategies to extend recyclability beyond ten cycles without loss of activity.

References

1. Amarasekara, A. (2024). *Advances in biomass-derived solid acid catalysts for green esterification*. Green Chemistry Reviews, 18(3), 245–268.
2. Chen, Y. (2023). *NMR markers for esterification monitoring: a molecular insight into alcohol-to-ester conversion*. Journal of Molecular Spectroscopy, 410, 112–120.
3. Chen, Z., Liu, H., & Patel, M. (2024). *Sulfonated lignocellulosic catalysts for bioderived ester synthesis: structure–activity relationships and kinetic optimisation*. Catalysis Today, 427, 89–104.
4. Jiang, X., Huang, H., & Liu, Y. (2025). *Heterogeneous sulfonated catalysts from biomass for esterification: mechanisms, diffusional effects and regeneration*. Renewable Catalysis Letters, 12(2), 55–72.
5. Kaur, R., Nahar, N., & Singh, S. (2020). *Bio-derived sulfonated carbon catalysts for esterification and transesterification*. Bioresource Technology Reports, 12, 100608.
6. Klemm, D., Heublein, B., Fink, H.-P., & Bohn, A. (2020). *Cellulose: structure, chemistry and applications*. Polymer Science Advances, 48, 112–130.
7. Li, X., Zhou, J., & Tan, X. (2021). *Surface sulfonation of cellulose fibres for catalysis and separation*. Carbohydrate Polymers, 255, 117388.
8. Lopes, M., Silva, F., & Duarte, R. (2023). *1H-NMR verification of ester conversion kinetics under green catalysis*. Journal of Organic Analytical Chemistry, 39(5), 52–61.
9. Mahmood, M., Rahman, Z., & Hussain, A. (2025). *Bio-sourced sulfonated catalysts: kinetic profiles, recyclability and process optimisation*. Sustainable Catalysis Engineering, 14(1), 33–59.
10. Niu, Y., Shi, H., & Li, Q. (2023). *One-step sulfonation of biomass fibres for high-activity green catalysts*. Journal of Cleaner Production, 412, 137056.
11. Pandey, R., Kumar, V., & Singh, P. (2022). *Oxidative activation pathways in cellulose functionalisation*. Carbohydrate Chemistry Annual Review, 58, 121–146.
12. Qiu, X., Zhang, H., & Sun, Z. (2023). *Structural effects in sulfonated biomass catalysts for esterification: morphology, acidity and mass transport*. Bioresource Catalysis Journal, 19(4), 115–128.
13. Tsubaki, A., Okada, T., & Ito, K. (2021). *Acid density evaluation of biosourced sulfonated catalysts: CHNS approach and catalytic implications*. Journal of Applied Polymer Chemistry, 138(21), 507–519.
14. Wang, G., Liu, F., & Zhao, T. (2022). *Morphostructural evolution during cellulose sulfonation and catalytic relevance*. Surface Engineering and Green Catalysis, 36(7), 441–457.
15. Wang, H., Chen, Z., & Feng, L. (2023). *Renewable sulfonated catalysts for esterification: mechanism, optimisation and stability*. Chemical Engineering Science, 274, 118–140.
16. Zhang, T., & Li, M. (2022). *Circular chemistry and biomass valorisation: emerging catalytic platforms*. Journal of Sustainable Chemistry, 17(2), 95–122.
17. Zhang, Y., & Wu, J. (2024). *1H-NMR-based validation of esterification products in catalytic systems*. Spectroscopy International, 12(3), 201–215.
18. Zhou, P., Wang, Y., & Huang, K. (2023). *Functional cellulose-based catalysts: structure–acidity optimisation for high-efficiency esterification*. Cellulose Chemistry and Applications, 30(6), 497–518.